# INFLUENCE OF THE SHIP'S LENGTH ON THE MANOEUVRABILITY IN A CANAL

Ir. E. LAFORGE; Flanders' Hydraulics, Antwerp, Belgium
Ir. P. CLAEYSSENS; University of Gent, Belgium
Prof. Dr. Ir. M. VANTORRE; University of Gent, Belgium

## ABSTRACT

The Port of Ghent (Belgium) is connected to the Scheldt Estuary by the Maritime Canal Ghent-Terneuzen (Fig. 1). The canal has a length of 32 km, 15.5 km of which are located on Dutch territory.

Originally, this canal was designed for 30 000 tdw vessels, but nowadays 80 000 tdw ships are allowed, provided that their dimensions do not exceed 256 m of length over all, 34 m of beam and 12.25 m of draught.

The Port of Ghent strongly insists on increasing the maximum allowed ship's length to 265 m, so that the Port would be accessible for all Panamax sized vessels. The passage of such ships through the lock at Terneuzen should not raise any major technical problems. There were fears that passage of longer vessels might cause problems due to the limited available width, especially at Sluiskil and at Sas van Gent where ships have to pass two long bends with a radius of 3000 m. Another reason for concern is the passage of three bridges.

A Committee of Dutch and Flemish Waterways and Marine Affairs Administrations agreed that a risk analysis was required in order to evaluate the differences in risk caused by allowing longer Panamax sized vessels ($L_{OA}$ = 265 m, B = 32.2 m, T = 12.25 m) to the canal. This study was performed by Flanders' Hydraulics, a research laboratory of the Ministry of the Flemish Community (Department of Environment and Infrastructure).

The work reported here involved:

- Systematic captive motion tests in the shallow water towing tank at Flanders' Hydraulics on three ship models, in open shallow water and in restricted water including a cross-section of the canal and a scale model of the geometry of the bends.
- Development of suitable mathematical models of the hydrodynamic forces for the three ships in open water and in the canal.
- Comparison of the behaviour of the three ships sailing along the canal through fast-time simulation. An autopilot, based on a cost-function concept, was used to perform the manoeuvring as it was expected that the variance between different pilots would mask differences between ships. Attention was paid to construct an auto-pilot unbiased with respect to the ship length.
- Evaluation of the results of the fast-time simulation.
- Validation of the autopilot runs through real-time simulation by experienced Terneuzen-Ghent Canal pilots on Flanders' Hydraulics manoeuvring simulator.

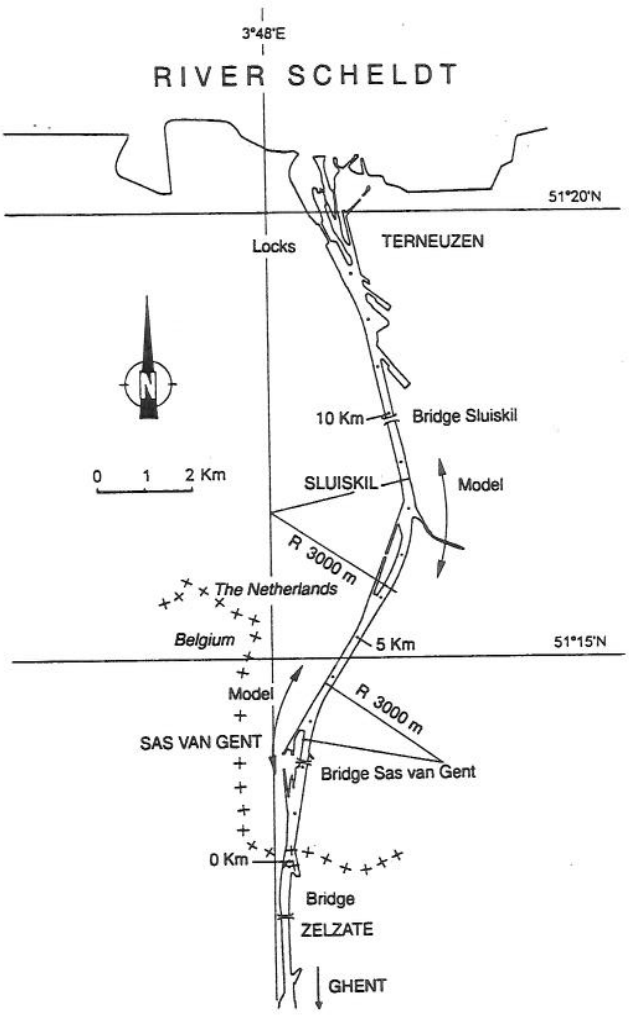


**Fig. 1 Situation.**

## EXPERIMENTAL PROGRAM

### Motivation

The development of a mathematical manoeuvring model which is able to simulate the passage of Panamax bulk carriers in the Maritime Canal from Terneuzen to Ghent is complicated by three factors.

- *Limited water depth to draught ratio*
  The depth of the standard cross-section of the canal is 13.5 m, while ships with a draught up to 12.25 m are allowed. This results in an under keel clearance of 10% of draught (h/T = 1.1), a condition for which reliable data are very scarce.
- *Restricted water effects.*
  The standard cross-section of the canal (Fig. 2) has a width at the bottom and at the waterline of 62 m and 155 m, respectively. The area of midship section of a typical ship with a beam of 32.2 m and a draught of 12.25 m takes about 27% of the cross-section of the canal. This configuration implies that forces due to blockage and to interaction with banks are expected to be of major importance.
- *Transient interaction phenomena.*
  The geometry of the canal at the bends (Fig. 1.) is particularly complex due to side branches connected to the canal, resulting into variations of width and cross-section. In these critical sections of the canal, the influence of varying blockage and ship-bank interaction effects on ship behaviour and controllability should be modelled in a reliable way.

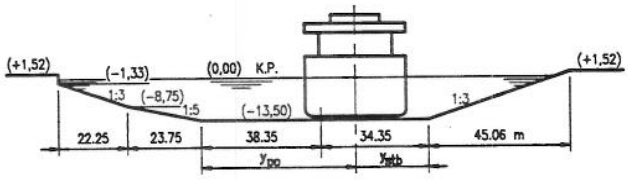


**Fig. 2 Standard cross-section.**

Insufficient data are available for simulating the combination of these three complicating factors, leaving the execution of tests involving scale models of ship and canal as the only possibility.

Due to the marginal difference between the actual allowed ship length (256 m) and the suggested maximum ship length (265 m), forces measured during captive tests with ship models of these lengths would lead to an unreliable comparison due to loss of precision during the procedure of fitting of experimental data to the mathematical formulations.

Therefore it was decided to perform a sensitivity analysis on three more different Panamax sized vessels with a length over all of respectively 230 m, 245 m and 265 m.

### Towing tank for manoeuvres in shallow water

*Background*

About ten years ago, most studies executed at Flanders' Hydraulics were hydraulic studies. Ever since, the laboratory is confronted more often with ship hydrodynamics and nautical problems. As a consequence, an extension of activities was esteemed necessary. This new approach led to the installation of a ship manoeuvring simulator (1989) and, as the study of ship behaviour in confined waters often requires model tests, the development of experimental facilities for ship models (1992-93). This *Towing Tank for Manoeuvres in Shallow Water (co-operation Flanders Hydraulics - University of Ghent)* was accepted as a ITTC member organisation in 1993. The facilities are described in detail in [1],[2].

At Flanders Hydraulics ship hydrodynamics are only investigated in relation with the design, renovation and operation of harbours, canals and fairways. This consideration resulted into two restrictions for the concept of the ship model facilities:

- water depth may be limited to about twice the maximum draught;
- only low model speeds have to be realised.

Priority was given to following research areas:

- determination of hydrodynamic coefficients occurring in the mathematical model of the ship manoeuvring simulator, with special attention for very restricted under keel clearance, lateral restrictions (banks), muddy bottoms, low speed (ahead and astern);
- vertical ship motions due to waves in shallow water.

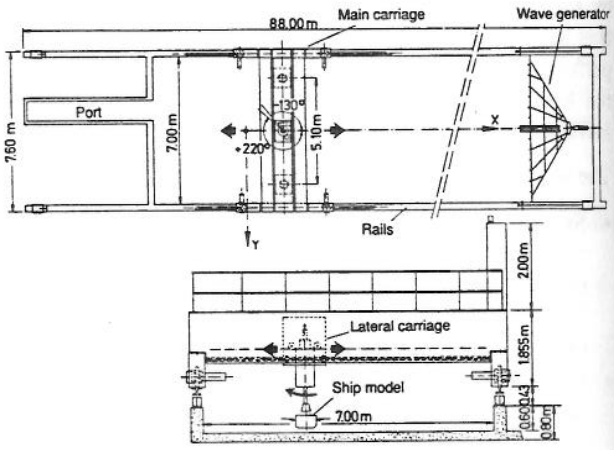


**Fig. 3 Shallow water towing tank.**

Summarising, the installation should allow the execution of captive manoeuvring and seakeeping tests in shallow water. Therefore, a towing tank was installed, equipped with a planar motion mechanism and a wave generator.

*Main characteristics* (Figure 3, Table 1)

Available space at Flanders Hydraulics allowed the construction of a 88 x 7 m² tank, with a useful length of 68 m. The latter is acceptable, as for manoeuvring tests ship models of about 4 m length are required, and one is mainly interested in low speed manoeuvres (<0.5 m/s). The height of the tank walls was chosen to be 0.60 m.

A computer controlled sway carriage - yawing table combination was preferred instead of a mechanical PMM. This offers more possibilities for studying several aspects of ship behaviour in restricted waters, such as forces acting on ships in parallel course with a bank or approaching a quay wall.

The maximum longitudinal velocity is sufficiently high compared with the economical speed of the ship models; at maximum speed, acceleration and deceleration zones both take 5 m. The characteristics of lateral carriage and yawing table allow harmonic oscillations with a track width of 5 m at minimal (tank resonance) period (12 s).

It is clear that the results of captive model tests are influenced by divergences between prescribed and actual trajectories performed by the ship model. This influence was studied theoretically ([3],[4]) in order to determine the accuracy requirements which should be met by the sub-mechanisms. Typically, position divergence's of 1.5 mm, 1.3 mm and 0.03°, and velocity errors of 0.5 mm/s, 1.7 mm/s and 0.08°/s were considered to be acceptable for the main carriage, the lateral carriage and the yawing table, respectively. With such an accuracy, the relative error due to control errors on the four main linear hydrodynamic derivatives should be less than 1% if the test parameters are chosen properly.

**Table 1. Range of positions, velocities and accelerations.**

| | longitudinal | lateral | rotation |
|---|---|---|---|
| min. position | 0.000 m | -2.550 m | -130.0 ° |
| max. position | 68.000 m | +2.550 m | +220.0 ° |
| min. velocity | 0.050 m/s | 0.000 m/s | 0.00 °/s |
| max. velocity | 2.000 m/s | 1.300 m/s | 16.00 °/s |
| max. acceleration | 0.40 $m/s^2$ | 0.70 $m/s^2$ | 8.00 $°/s^2$ |
| power | 4 x 7.2 kW | 4.3 kW | 1.0 kW |

*General layout*

The tank is composed of reinforced concrete sections, connected by joints. Foundations were not required due to the presence of underground reservoirs. The tank bottom was levelled with an accuracy of ±1 mm, which is required for tests in shallow water. The upper and, at one side, lateral surfaces of the rails are milled and finished. They are aligned with high accuracy: level differences and lateral deflections are less than 0.5 mm.

The main carriage is as a rectangular frame, composed of two wheel girders, connected by means of two box girders. The four wheels are driven by brushless AC-servo-motors by way of a gearing. The position of the carriage is determined separately by a measuring wheel.

The lateral carriage, which carries the yawing table, is guided between the transversal girders and driven by a servomotor by way of a planet gear and a pinion-rack combination.

The vertical rotation tube is incorporated in a slide which can be positioned manually in vertical sense, and is driven by a servomotor by way of a reducer with large ratio (1:320) and restricted backlash. The tube is attached to the ship model by means of a beam and a mechanism allowing free heave and pitch, but creates a rigid connection in other modes.

*Control and data-acquisition*

The three motion modes, as well as three analog and four digital outputs for activating rudder, propulsion and auxiliary devices, are controlled by a personal computer.

All information required for execution of a captive test is stored in a trajectory file, which contains a sequence of reference values for the sub-mechanism positions and for the analog and digital outputs. Based on this file, reference values for the velocity of the sub-mechanisms at each point of time are calculated and stored into the controller memory. The time increment is a multiple of 25 ms, the maximum number of points being 7000.

During the test, the controller sends reference signals to the servo amplifiers which control the velocity of the respective motors by means of a PI-control system. The position of the submechanisms is fed back to the controller, which adapts the velocity reference signals to the trajectory errors by means of digital PID-filters.

The test sequence can be determined by means of a batch file. This option allows unmanned operation, so that experiments can be carried out 24 hours a day, 7 days a week.

A second computer samples successively 24 analog input signals with a variable sample frequency up to 40 Hz. During captive manoeuvring tests, following data are measured and stored digitally (see figure 4):

- position of sub-mechanisms
- longitudinal force (fore and aft)
- lateral force (fore and aft)
- sinkage (fore and aft)
- propeller characteristics (rpm, thrust, torque)
- rudder characteristics (deflection, longitudinal and lateral force components, torque).

Ship Models

A scale of 1:64 was selected, taking account of following considerations:

- the ship model length should be about 4 m;
- the canal model should fit into the towing tank.

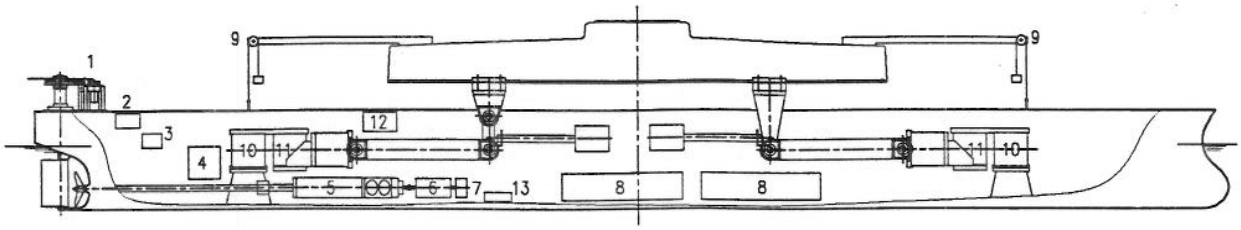


1 Rudder mechanism
2 Electronic rudder control
3 Bilge pump
4 Bilge pump battery
5 Propeller thrust and torque transducer
6 Propeller drive
7 Propeller speed
8 Amplifier
9 Sinkage transducer
10 Longitudinal force transducer
11 Transverse force transducer
12 Propeller control
13 Water leak security

**Fig. 4 Ship model and instrumentation.**

In order to obtain three ships with comparable lines but varying length, a ship model was assembled with a fore section and an aft section for the shortest ship (230 m full scale), alongated byone of two prismatic midsections for the longer ships (245 m and 265 m full scale).

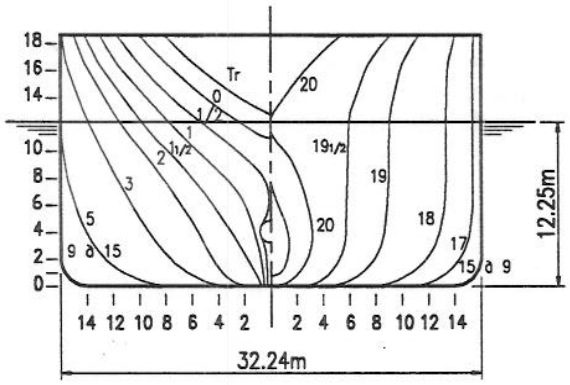


**Fig. 5 Ship body plan.**

The lines of these sections were based on an existing ship hull with $L_{OA}$ = 241 m (see figure 5). Each ship model was fitted with a separate rudder, so that the lateral rudder area equals 0.016 $L_{PP}T$. The same propeller ( Wageningen B4-62, P/D=0.65, D=6.64 m) was mounted on all ship models. Characteristic model dimensions are mentioned in Table 2.

Scale Model of the Canal

Captive model tests were executed with the three ship models mentioned above in following geometric configurations:

(a)in open shallow water (h/T = 1.1);
(b)in a standard cross-section of the canal;
(c)in a model of the bends at Sluiskil and at Sas van Gent, connected with a standard cross-section (Fig. 6).

Due to the limited width of the towing tank, the bends of model (c) had to be straightened. This is justified, as the only purpose of captive tests in this geometry consists of measuring the ship-bank interaction forces due to variations of the canal's cross-section. Taking account of the magnitude of the rate of turn, which is 0.05°/s for a ship moving at a speed of 2.5 m/s on a circle with a 3000 mradius, it is expected that forces and moments due to the curved, path are negligible compared to ship-bank interaction forces.

**Table 2. Main dimensions**

| parameter | full scale | model |
|---|---|---|
| length over all | 265 /245 / 230 m | 4.141 /3.828/ 3.594 m |
| beam | 32.4 m | 0.506 m |
| draught | 12.25 m | 0.1914 m |
| block coefficient | 0.81/0.83/0.84 | 0.81/0.83/0.84 |
| water depth | 13.50 m | 0.2109 m |
| underkeel clearance | 1.25 m | 0.0191 m |
| width towing tank | 448 m | 7.00 m |
| ship speed | 9 km/h (2.5 m/s) | 0.32 m/s |
| tug bollard pull | 20 tonf | 1.05 N |

The length of the standard cross-section connecting the two bends in model (c) was about 4 ship lengths, which appeared not to be completely sufficient for eliminating transient phenomena. For this reason, tests were also executed in model (b), with a length of about 8 ship lengths.

## EXPERIMENTAL RESULTS

Open shallow water

It is known that a ship's manoeuvrability and controllability depends very much on water depth. From a ship hydrodynamics point of view, an under keel clearance of 10% of draught, which is common practice in protected inner waterways and harbours, should be considered as an extreme condition. Some typical shallow water effects are mentioned below.

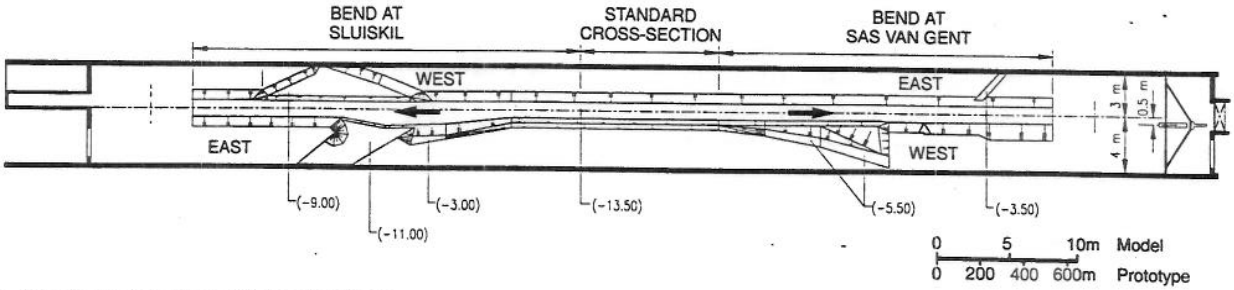


**Fig. 6 Scale model of canal in towing tank.**

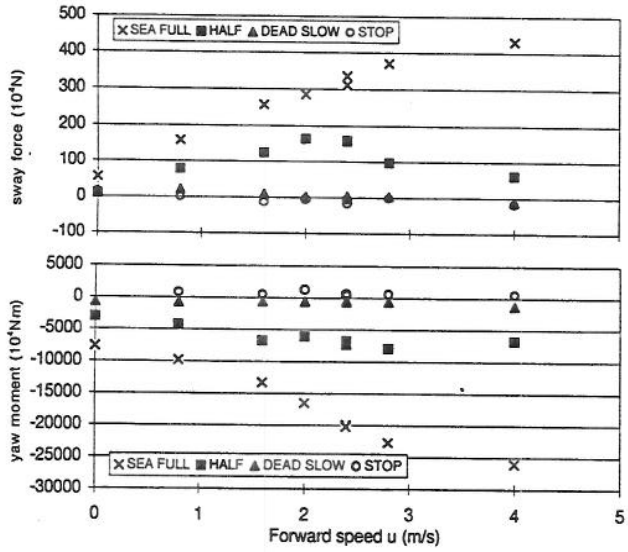


**Fig. 7 Open water results. Ship 265 m: $\beta$=0., $u$=2.4 m/s, $\delta$=30°**

- *Inertia forces and moments.* The added mass for sway ($Y_v$) and the added mass moment of inertia ($N_r$) appear to take values of about 2.5 to 3 times the ship's mass and the ship's moment of inertia, respectively, which is significantly more than in deep water. A ship will therefore be more sluggish in her reactions to rudder action and to external disturbances.
- *Sway and yaw* induced stationary forces and moments increase with decreasing water depth.
- Lateral forces induced by *rudder action* increase significantly in shallow water. This effect is not caused by an increase of the forces acting on the rudder itself, but can be explained by an increase of the force acting on the hull due to the asymmetry caused by the rudder deflection. The magnitude of this rudder induced hull force, which takes values from 20 to 40 % of the lateral force acting on the rudder in deep water, appears to exceed the latter 2 to 3 times at h/T = 1.1 [5].
  The effect of this increased rudder induced hull force on the yawing moment is rather limited, as the application point appears to be situated near the midship section.
- The *wake factor*, taking a typical value of 0.3 in deep water, appears to increase to about 0.9 at an under keel clearance of 10% of draught. As a result, the flow to the rudder is heavily obstructed, so that propeller action is required in order to use the rudder in an efficient way (see fig. 7).

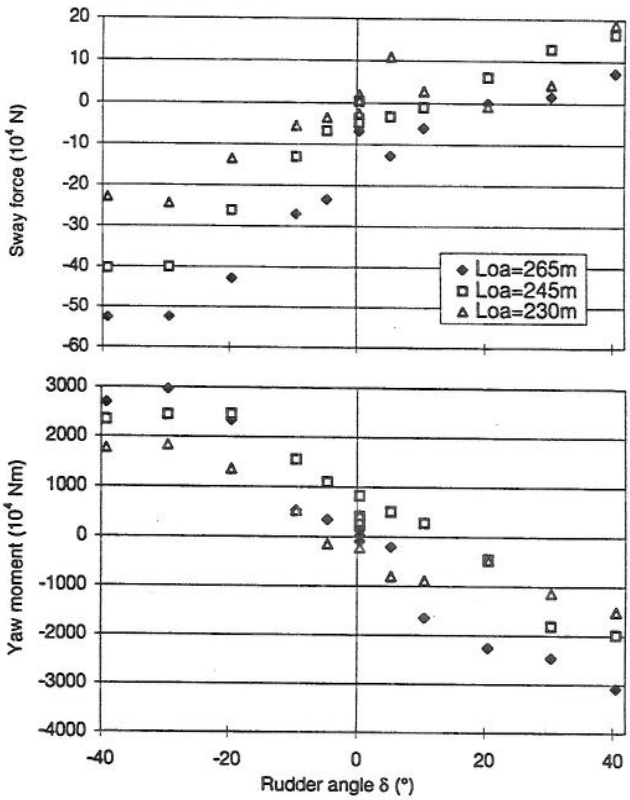


**Fig. 8 Open water results. u=2.4 m/s, n= 50 rpm, δ=0.**

The influence of the ship's length on hydrodynamic forces can be summarised as follows.

- It is clear that sway and yaw induced stationary forces and moments increase with ship length.
- Rudder induced forces also increase with ship length. This is only partially due to the increased rudder surface, as the increase of the rudder induced hull force is relatively larger and it application point is situated more aft. As a result, the rudder induced yawing moments increase by about 25% for a 15% increase in ship length (fig. 8).

In order to illustrate the influence of ship length on manoeuvrability, characteristics of simulated turning circles are given in Table 3. The tactical diameter takes values between 6.9 and 8.8 ship lengths. It is surprising that, probably due to increased rudder induced forces, this diameter decreases slightly with increasing ship length.

**Table 3 Turning circles.**

| | Loa=265m | Loa=245m | Loa=230m |
|---|---|---|---|
| advance (m) | 1060 | 1096 | 1119 |
| transfer (m) | 900 | 950 | 996 |
| tactical diameter (m) | 1823 | 1936 | 2030 |
| starting speed (m/s) | 2.4 | 2.4 | 2.4 |
| speed in steady turn (m/s) | 2.18 | 2.24 | 2.32 |
| propeller speed (rpm) | 50 (half) | 50 (half) | 50 (half) |
| steady drift angle (°) | 2.1 | 1.9 | 1.5 |

Canal Standard Cross-Section

Hydrodynamic forces acting on the ship are influenced by the presence of the canal banks due to two effects:

- bank effects, caused by asymmetric flow;
- blockage effects, caused by backflow.

*Bank effects* depend on a number of parameters :

- Ship speed.
- Under keel clearance. Especially in very shallow water, interaction effects are very sensitive to depth variations. If *h/T* exceeds a critical value, a ship moving in parallel course with a bank with stopped propeller is attracted to the nearest bank, while at lower *h/T*, repulsion from the bank occurs. The critical depth-to-draught ratio varies between *1.1* and *1.3*, according to data in [6] and [7]. Test results pointed out that critical conditions were reached in the present configuration. Yawing moments $N_{rest}$ always tend to attract the stern to the nearest bank, and increase substantially with decreasing water depth.
- Propeller thrust. A positive propeller rpm results in an attraction between the stern and the nearest bank. As a result, bank repulsion occurring at small under keel clearance if the propeller is stopped can be changed into bank attraction due to this effect.
- Lateral position, expressed by means of an undimensional parameter $y_b$ [6]:

$$y_b = \left(\frac{1}{y_s} + \frac{1}{y_p}\right)\frac{B}{2}$$

- In Fig. 9, the lateral bank interaction force $Y_{rest}$ is compared with forces caused by rudder action, illustrating that the latter are not able to compensate bank suction if $|y_b| > 0.3$.

Ship-bank interaction forces increase with ship length. At the self-propulsion point, a 15% increase of length results into an increase of $Y_{rest}$ and $N_{rest}$ of 10% and 50%, respectively, for $y_b = 0.3$. On the other hand, the increase of rudder induced forces is relatively larger.

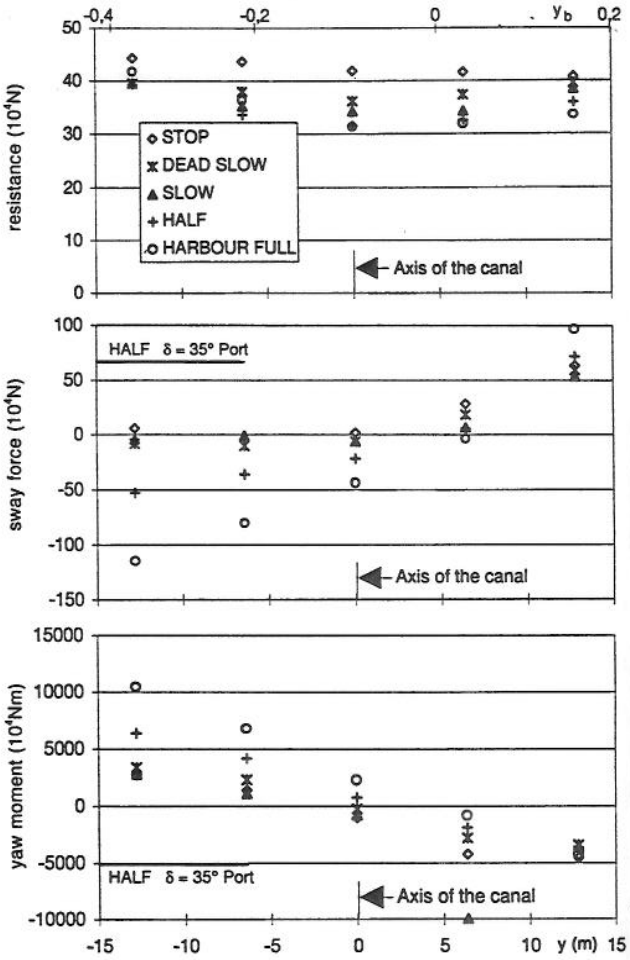


**Fig. 9 Ship-bank interaction forces. ship 265 m, u=2,56 m/s, β=0°, δ=0°**

*Blockage effects:*

At maximum allowed ship speed in the canal (2.4 m/s), resistance increases by 70% due to blockage effects. Another 30% increase in resistance was measured when sailing closer to the banks ($y_b$ going from 0 to 0.3).

Drift forces in the standard cross-section doubled compared to open shallow water due to blockage effects. A 15 % increase in ship length results in a 50 % rise in yaw moment and 20 % rise in sway force for small drift angles in the standard cross section.

Rudder forces increase by approximately 30% in the standard cross section compared to shallow open water.

Bend Sections

Sailing through the Sluiskil and Sas van Gent model sections interaction forces up to 5 times the mean value in the standard cross-section were measured due to transient phenomena. An illustration of the complex behaviour is given in Fig. 10.

Special observations

During stationary test an oscillatory behaviour of the lateral forces on the ship without any obvious reason was

observed. The fluctuations were most pronounced on the lateral force at the bow. At 20 % under keel clearance the fluctuations almost disappeared, so it was concluded that this was an hydrodynamic phenomenon due to the small under keel clearance. The origin of the phenomenon is not clear.

- Wave resonance in the towing tank was found not to be involved.
- Increasing the waiting time between two experiments from 25 to 45 minutes had only little effect; the motion in the tank after 25 minutes is of the order of a few mm/s (a few cm/s full scale) and dies out very slowly.
- Visualisation of the flow field around the hull showed a turbulent flow pattern, eliminating a possible laminar flow effect. The flow tends to oscillate between starboard or port side at a distance of about 10% of *Lpp* in front of the bow.
- Norrbin [8],[9] states that the problem may be attributed to flow separation originated on the bulbous bow. Visualisation of the flow around the bulbous bow was not conclusive.

Fortunately, the average forces seemed not to be influenced by these turbulence: in the correlation between forces and speed, propeller rate, drift angle etc. no deviations could be seen.

## MATHEMATICAL MODELLING

### General formulation

The mathematical model was designed on the grounds of three considerations: theoretical background, existing mathematical models and analysis of the measured data.

The basic mathematical model is the application of Newton's second law written in a ship bound moving co-ordinate system and has the following general form:

$$\begin{cases} m(\dot{u} - vr - x_G r^2) = X_{hull} + X_{prop} + X_{rud} + X_{wind} + X_{restr} \\ m(\dot{v} - ur + x_G \dot{r}) = Y_{hull} + Y_{prop} + Y_{rud} + Y_{wind} + Y_{restr} \\ I_{zz}\dot{r} + mx_G(\dot{v} + ur) = N_{hull} + N_{prop} + N_{rud} + N_{wind} + N_{restr} \end{cases}$$

Modelling of hull, propeller, rudder and restricted water forces is based on the captive motion tests. Most forces are expressed in a polynomial form where each term is preceded by a coefficient that is determined on the basis of the captive motion tests. The parameters in these formulae are the velocity and acceleration components $u, v, r, \dot{u}, \dot{v}, \dot{r}$, lateral position $y$, rudder angle $\delta$ and propeller speed $n$. The form of the model is the same for each ship but the coefficients will change. Themathematical model was largely based on curve fitting methods because existing models or theoretical assumptions were found to be inaccurate or inadequate.

### Open Water

The mathematical model for open water consists of components for hull, rudder and propulsion. Formulations are given for the propeller turning ahead only.

Hull forces are

$$\begin{cases} X_{hull} = X_{uu}u|u| + X_{rr}r^2 + X_{uvr}uvr + X_{\dot{u}}\dot{u} + X_{vv}v^2 \\ Y_{hull} = Y_{uv}|u|v + Y_{vv}v| + Y_{ur}ur + Y_{r|r|}r|r| \\ \qquad + Y_{r|v|}r|v| + Y_{|r|v}|r|v + Y_{\dot{v}}\dot{v} + Y_{u\dot{v}}u\dot{v} + Y_{\dot{r}}\dot{r} \\ N_{hull} = N_{uv}|u|v + N_{vv}v|v| + N_{ur}ur + N_{r|r|}r|r| \\ \qquad + N_{r|v|}r|v| + N_{|r|v}|r|v + N_{\dot{v}}\dot{v} + N_{\dot{r}}\dot{r} \end{cases}$$

Propulsion forces are

$$\begin{cases} X_{prop} = X_{nn}n^2 + X_{nu}nu \\ Y_{prop} = Y_{vn}vn \\ N_{prop} = 0 \end{cases}$$

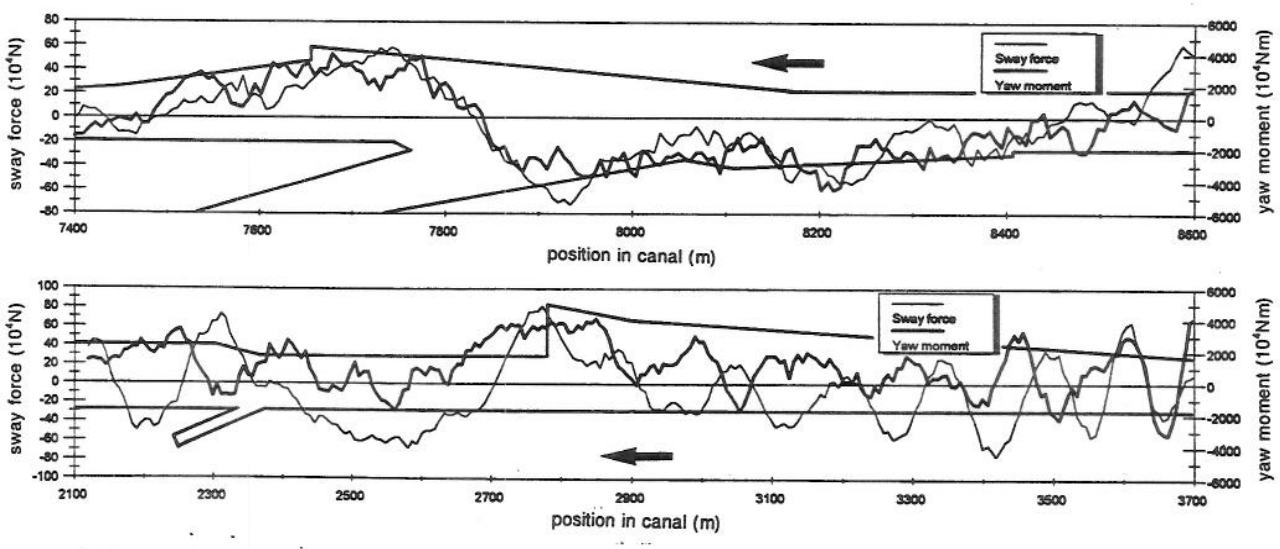


**Fig. 10 Ship-bank interaction in bend section. Ship 265 m. u=2.4 m/s, δ=0°, β=0°, n=0 rpm.**

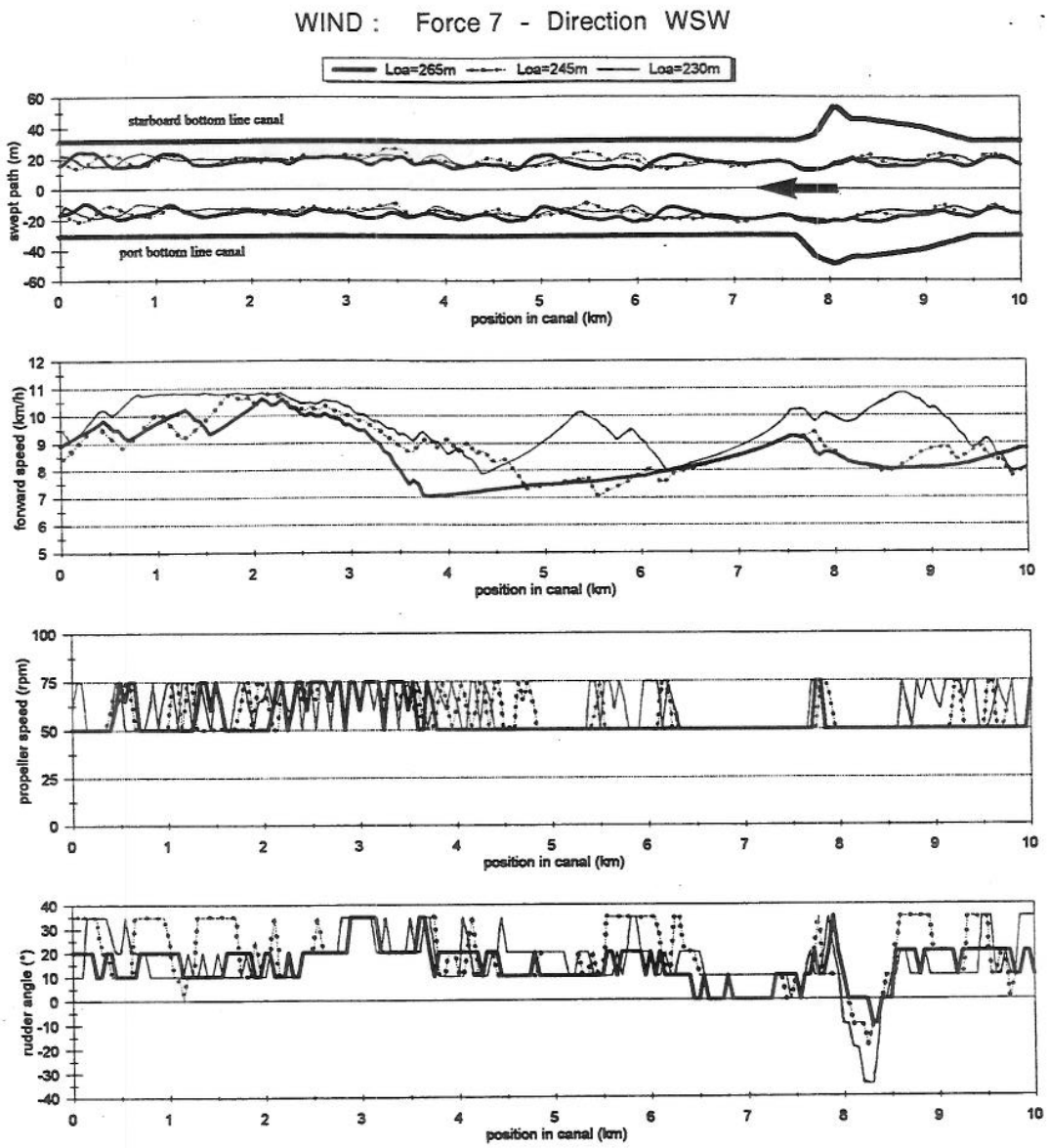


**Fig. 11 Example of a fast-time simulation result.**

Rudder forces are

$$\begin{cases} X_{rud} = X_{\delta\delta uu}\delta^2 u^2 + X_{\delta\delta un}\delta^2 un + X_{\delta\delta nn}\delta^2 n^2 \\ Y_{rud} = Y_{\delta u|v|}\delta u|v| + a_Y.\{Y_{\delta un}\delta un + Y_{\delta nn}\delta nn \\ \quad + Y_{\delta\delta nn}\delta^2 n^2 + Y_{\delta\delta\delta nn}\delta^3 n^2\} \\ N_{rud} = N_{\delta u|v|}\delta u|v| + a_N.\{N_{\delta un}\delta un + N_{\delta uu}\delta uu \\ \quad + N_{\delta\delta\delta nn}\delta^3 n^2\} \\ a_Y = 1 \quad \text{if } \frac{u}{nD} < Y_{Jmax}, \text{ else } a_Y = 0 \\ a_N = 1 \quad \text{if } \frac{u}{nD} < N_{Jmax}, \text{ else } a_N = 0 \end{cases}$$

Restricted-Water Effects in Standard Cross-Section

For the longitudinal forces back flow effects are taken into account by adding the back flow speed to the speed of the ship over the ground in the open water model:

$$\begin{cases} X_{prop} = X_{prop,open}\left(u.\frac{A_c}{A_c - B.T}\right) \\ X_{rud} = X_{rud,open}\left(u.\frac{A_c}{A_c - B.T}\right) \end{cases}$$

The restricted-water forces are

$$\begin{cases} X_{restr} = X_{trnn}n^2 \\ Y_{restr} = Y_{tuu}u^2 + Y_{tvu}vu + Y_{tv|v|u}v|v|u + Y_{bu|u|}y_b u|u| \\ \quad + Y_{brnn}y_b n^2 + Y_{\delta nn}\delta n^2 + Y_{trnn}n^2 + Y_{t\delta nnn}\delta n^3 + Y_{bru}y_b ru \\ N_{restr} = N_{tuu}u^2 + N_{tvu}vu + N_{tv|v|u}v|v|u + N_{bu|u|}y_b u|u| \\ \quad + N_{brnn}y_b n^2 + N_{t\delta nn}\delta n^2 + N_{trnn}n^2 + N_{t\delta nnn}\delta n^3 + N_{bru}y_b ru \end{cases}$$

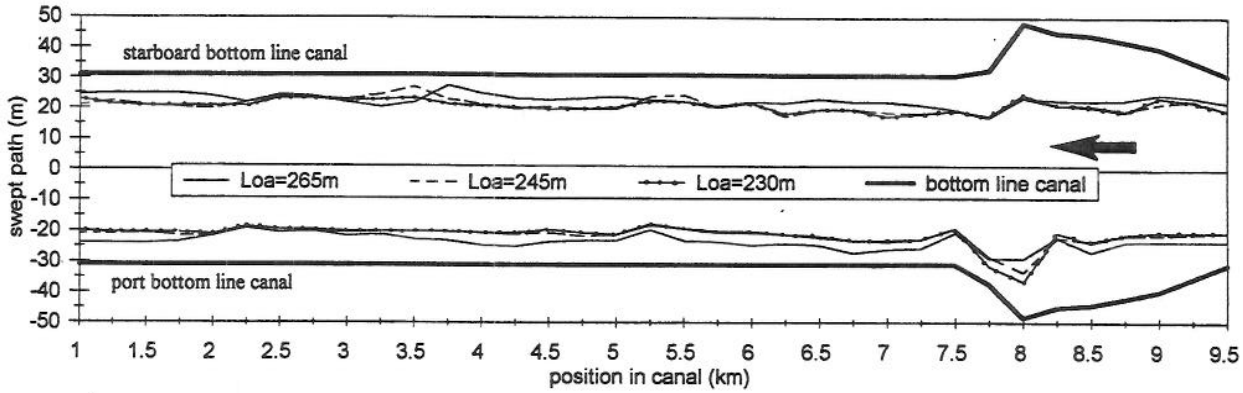


**Fig. 12 Swepth path : probability of exceedance of 0.01%**

Restricted-Water Effects in the Bend Sections.

After reduction of the net interaction force data for the influence of lateral position, speed, propeller rate and rudder angle, the remaining fluctuations due to the changes in canal geometry and to the drift angle of the ship could not accurately be moulded into a mathematical formula.

For this reason the net interaction forces for the ship sailing at the maximum allowed speed ($u_{max} = 2.4\ m/s$) in the middle of the canal ($y = 0$), with zero rudder angle $\delta$ and zero propeller speed $n$ are tabulated for drift angles $\beta$ of -5°,-2.5°, 0°, 2.5° and 5° as function of the distance $s$ in $X_{table(\beta,s)}$, $Y_{table(\beta,s)}$, $N_{table(\beta,s)}$. Different tables are needed for each ship and each direction of passage.

The influence of lateral position, rudder angle and propeller speed is expressed as follows:

$$\begin{cases} X_{restr} = \left(\dfrac{u}{u_{max}}\right)^2 X_{table}(\beta,s) \\ Y_{restr} = \left(\dfrac{u}{u_{max}}\right)^2 Y_{table}(\beta,s) + Y_{byyy}\, y^3 + a_1\, Y_{snn}\, n^2 \\ \qquad + a_2\, Y_{b\delta n} \dfrac{\mathrm{sgn}(\delta).\min(|\delta|,20.)}{n} \\ N_{restr} = \left(\dfrac{u}{u_{max}}\right)^2 N_{table}(\beta,s) + N_{byyy}\, y^3 + a_1\, N_{snn}\, n^2 \\ \text{with} \\ a_1 = 1 \text{ if } n > 0 \text{ else } a_1 = 0 \\ a_2 = 1 \text{ if } \dfrac{\delta}{n} > 0.15 \text{ else } a_2 = 0 \end{cases}$$

The restricted-water forces at the transition from the bend section to the standard cross section were interpolated between the two formulations over one ship's length.

## FAST TIME SIMULATION PROGRAM

Development of an Autopilot

For the comparison of the three ships a number of simulation runs for a large spectrum of wind conditions had to be carried out. The difference in swept path between the three ships is based on a statistical study of all runs.

Based on the experience on the simulator at Flanders' Hydraulics it is known that differences in the execution of the same manoeuvre by pilots can be quite large. It was feared that the differences in swept path between the three ships would be masked by human variance. Therefore it was decided to use a steering automaton to make comparable runs with the three ships for the same wind condition . The autopilot has to be unbiased with respect to the ship length.

Most of the autopilots on board of ships consist of a PID-controller. A PID controller with constant coefficients wasfound to be unable to keep the ship on its course in the canal [10]. For the unbiased autopilot a coarse version of the mathematical model of each ship is used to predict the ship's position for different rudder angles after a short lapse of time. The optimum rudder command is the one that will minimise a cost function of the ships predicted position. The cost function includes the distance of the ship's stern, midpoint and bow relative to the trajectory that has to be followed. The cost function was identical for all three ships.

In order to give the autopilot a human touch rudder commands are limited to 0, 10, 20 or 35° to either port or starboard side. The rate of propeller revolutions is limited to those corresponding with the settings of the ships telegraph.

The autopilot calculates every 10 seconds the different trajectories corresponding to the rudder commands and a higher or lower telegraph commands. Changes of the propeller rate are limited to 30 seconds as not to accelerate the ship beyond the speed limit on the canal.

The autopilot performed satisfactory and lost only once control of the 245 m long ship at a force 7 westerly wind condition in the bend near Sas van Gent.

Test program.

A fast time simulator program was adapted to the use of the new autopilot. Position, course, speed as well as rudder angle and propeller rate were filed for further analysis.

Wind data measured between 1986 and 1989 at Ertvelde (near the canal) were used. From these data 107 different wind conditions were used with wind speed from 0 to 7 Beaufort in combination with wind directions over 360° with a step of 22.5°. The wind turbulence is simulated by the use of a von Karman spectrum. Care was taken to use the same time history of turbulence for the corresponding runs of the three ships.

An example of a autopilot run for each ship is given in Fig. 11.

Results

*Use of rudder and propeller speed:*

- If the wind speed is higher than 5 Beaufort the use of the rudder increases fast; below that speed ships are rather insensitive to the wind.
- Intensive rudder action is required when the wind is perpendicular to the canal (a south east to north west wind, the most common wind directions).
- In comparison with actions taken by pilots, the autopilot's rudder action is less nervous and the absolute values are smaller.
- Telegraph orders are systematically given at certain difficult positions in the canal, for example coming out of the Sas van Gent bend.
- the wind seems to have a larger influence on the shorter ships, which results in more frequent use of propeller thrusts.

*Ship Speed*

The speed variations are similar for the three ships. The average ship speed will be less for the longer ships due to increased resistance as the three ships are using the same propeller. Because shorter ships take more often propeller actions, the difference in forward ship speed at the critical positions in the canal can be more important.

The ship's speed does not exceed the speed limit of 9 km/h for wind speeds under 19 knot (force 5). Once the wind speed exceeds the 19 kn. limit, especially for westerly winds, the forward ship speed may exceed the speed limit due to propeller action.

## EVALUATION OF THE SWEPT PATH

Method

In cross-sections every 50 m along the canal, the distance from the axis of the fairway to the outermost points of the hull of the passing ship were recorded. With the 107 runs histograms for the left bank and for the right bank are constructed for each group of five sections (every 250 m over 9 km; with 535 data points each).

Because the risk analysis has to take into account the combination of the probability of the ship exceeding a certain distance for one wind condition with the probability of occurrence of this wind condition, the histogram was constructed by calculating the frequency of each class not as the number of occurrences but as the sum of the probabilities of occurrence at Ertvelde of the wind conditions.

Based upon these distributions the distances corresponding with probabilities of 10, 1, 0.1, 0.01 and 0.001% per year were interpolated and plotted along the canal as shown in Fig. 12. The longest ship not always needs the largest swept path. The position where the maximum swept path occurred was near the end of the bend at Sas van Gent for all ships.

The width of the swept path was calculated by adding the distances on each side of the centerline. The difference in swept path is summarised by looking at the average width for each ship for the probabilities mentioned above.

**Table 4.** Average swept path (m)

| | probability of exceedance (%) | | | | |
|---|---|---|---|---|---|
| $L_{OA}$ | 10 | 1 | 0.1 | 0.01 | 0.001 |
| 265 m | 40.5 | 44 | 45.9 | 46.6 | 46.9 |
| 245 m | 38.4 | 40.4 | 41.7 | 42.7 | 43.9 |
| 230 m | 38 | 39.9 | 41.0 | 42.3 | 43.3 |

**Table 5.** Maximum swept path (m)

| | probability of exceedance (%) | | | | |
|---|---|---|---|---|---|
| $L_{OA}$ | 10 | 1 | 0.1 | 0.01 | 0.001 |
| 265 m | 48.3 | 50.3 | 51.3 | 52.8 | 52.8 |
| 245 m | 47.8 | 59.3 | 53.3 | 57.3 | 59.8 |
| 230 m | 47.8 | 51.8 | 56.8 | 61.3 | 64.8 |

Results

It was found that the expected average swept path increases with increasing ship length (Table 4).

By interpolation between the two largest ships a value for the 256 m long reference ship was calculated. In Fig. 13 the difference is shown to be 4%, being about 1.8 m.

The maximum value along the canal of the swept path for each probability value was tabulated. These maxima decrease with increasing ship length (Table 5, Fig. 14). The greater inertia with respect to fluctuating wind and interaction forces can be the reason for this result.

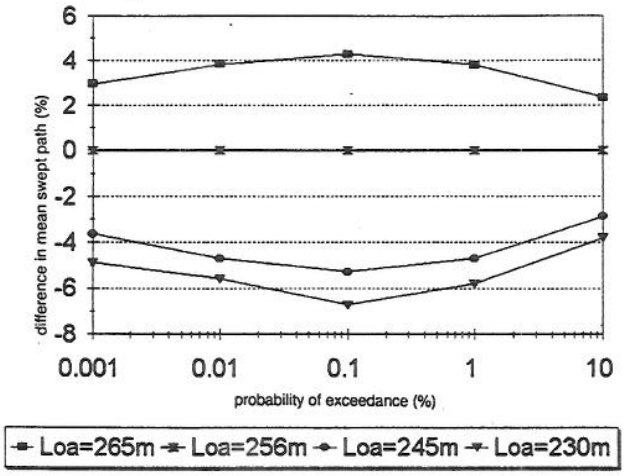


**Fig. 13 Difference in expected mean swept path**

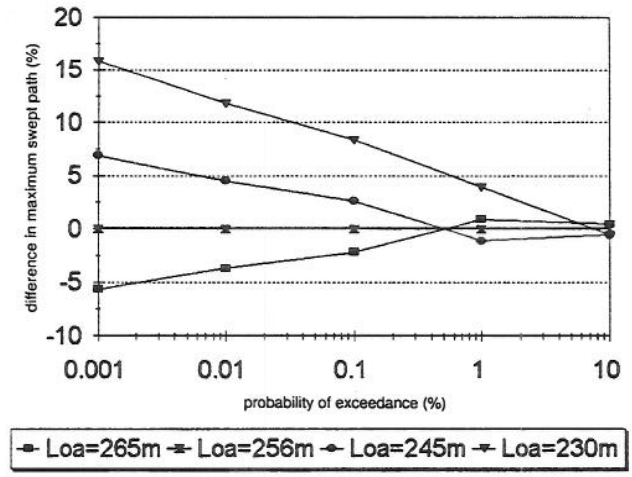


**Fig. 14 Difference in expected maximum swept path.**

The difference between the distance to the toe of the banks of the 265 m versus the 245 m ship was also calculated at each cross-section for each run. The mean difference of these paired distances for the larger ship was found to be +0.26 m for portside and -0.61 m for starboard side, while the standard deviation was around 2.9 m. The distribution of the differences was normal. From this fact it was concluded that this difference was not significant.

Sensitivity.

To give some idea about the importance of a change in ship length in relation to other ships properties, the comparison was repeated for ships with a 20% larger and 20% smaller rudder.

As seen in Table 6 the increase of the average swept path for a ship with a rudder that has a 20% smaller surface equals the difference in average swept path between the ships with $L_{OA}$=265m and $L_{OA}$=230m. Larger rudders give only small improvements to the swept path.. Differences in course stability were also tested by changing the $Y_{ur}$ and $N_{ur}$ coefficients resulting in small differences (ca 1 m) for the average swept path..

**Table 6.** Comparison of differences in expected mean swept path (m)

| | probability of exceedance (%) | | | | |
|---|---|---|---|---|---|
| | 10 | 1 | 0.1 | 0.01 | 0.001 |
| + 45 m length | 2.5 | 4.0 | 4.2 | 2.7 | 0.4 |
| -20% rudder | 2.5 | 4.1 | 4.9 | 4.3 | 3.6 |

## VALIDATION BY REAL-TIME SIMULATION

After the autopilot runs, the mathematical model was implemented on the ship manoeuvring simulator at Flanders' Hydraulics. A description of this facility is given in [11],[12]. Databases for radar and scenery were prepared. Simulation runs were executed by experienced canal-pilots, asked to keep the ship on the canal centerline. In their comments they confirmed the good similarity between simulation and reality for the ship and the bank suction effects at Sluiskil. In the opinion of some pilots the suction effects at Sas van Gent deviated from reality. This can be explained by the difference between the theoretical (design) cross-section of the canal adopted in this study and the actual section..Also some pilots kept strictly to the centerline of the fairway, some tried to use bank suction effects in the bends by approaching the bank, e.g. to line up for the bridge at Sas van Gent.

The real-time simulations confirm the fast-time simulations.

## CONCLUSIONS

For this study intensive measurements on scale models were performed to allow a high degree of accuracy in the consecutive mathematical modelling. Notwithstanding the differences in the behaviour of the ships only small differences in swept path are found when sailing under the control of a feedback loop such as an autopilot, that can take the fluctuating bank effects into account.

As a result the difference between the expected swept paths calculated corresponding the wind frequency data of the 265 m long ship with respect to the 256 m reference ship is estimated to be 4% [13].

## ACKNOWLEDGEMENTS

The permission granted by the Director-general of the Administration of Waterways and Marine Affairs of the Ministry of the Flemish Community to publish this paper is fully appreciated by the authors.

## SYMBOLS

| | |
|---|---|
| $L_{OA}$ | length over all (m) |
| $L_{PP}$ | length between perpendiculars (m) |
| $h$ | water depth (m) |
| $T$ | draught (m) |
| $B$ | beam (m) |
| $m$ | mass of the ship (kg) |
| $A_c$ | cross-section area of canal ($m^2$) |
| $u$ | ship longitudinal velocity (m/s) |
| $v$ | sway velocity(m/s) |
| $r$ | yaw velocity(rad/s) |
| $\dot{u}$ | surge acceleration($m/s^2$) |
| $\dot{v}$ | sway acceleration($m/s^2$) |
| $\dot{r}$ | yaw acceleration($rad/s^2$) |
| $n$ | propeller speed (rpm) |
| $\delta$ | rudder angle (rad) |
| $\beta$ | drift angle (rad) |
| $y_b$ | bank-distance parameter |
| $y_s$ | distance from the ship's centreline to the toe of the bank at starboard side (m) (starboard positive) |
| $y_p$ | distance from the ship's centreline to the toe of the bank at port side (m) |
| $x_G$ | distance between the centre of gravity of the ship and the middle of the ship (m) |
| $I_{zz}$ | moment of inertia around vertical z-axis through the centre of gravity of the ship ($kgm^2$) |
| $X$ | surge force (N) |
| $Y$ | sway force (N) |
| $N$ | yaw moment (Nm) |
| $Y_{Jmax}$ | critical advance coefficient for the rudder sway force |
| $N_{Jmax}$ | critical advance coefficient for the rudder yaw moment |
| $X_{uu}...X_{\delta\delta nn}$ | surge force coefficients in open water |
| $Y_{uv}...Y_{\delta\delta\delta nn}$ | sway force coefficients in open water |
| $N_{uv}...N_{\delta\delta\delta nn}$ | yaw moment coefficients in open water |
| $X_{tnn}$ | surge force coefficients in standard cross section |
| $Yt_{uu}..Yt_{\delta nnn}$ | sway force coefficients in standard cross section |
| $Nt_{uu}..N_{t\delta nnn}$ | yaw moment coefficients in standard cross section |
| $Y_{snn}$ | sway force coefficients in bend sections |
| $Y_{snn}$ | yaw moment coefficients in bend sections |

## REFERENCES.


[1] VANTORRE, M.; LAFORCE, E. "Manoeuvring Simulation and model tests for safe shipping traffic". Ghent werkt/works, December 1992, nr. 93, pp. 51-55.

[2] VANTORRE, M. "Concept and operation of a computer controlled towing tank for manoeuvres in shallow water". In: Marine, Offshore and Ice Technology, CADMO'94 and ITC'94, Southampton, September 1994), Editors: MURTHY, T.K.S.; WILSON, P.A.; WADHAMS, P. Computational Mechanics Publications, Southampton/Boston, pp. 123-132, 1994.

[3] VANTORRE, M. "Accuracy considerations and optimisation of parameter choice for captive manoeuvring tests with ship models" (in Dutch). D.Sc. Dissertation, Faculty of Applied Science, University of Ghent, December 1989.

[4] VANTORRE, M. "Accuracy and optimisation of captive ship model tests". In: (5th International Symposium on) Practical Design of Ships and Mobile Units (Newcastle upon Tyne, May 1992), Editors : CALDWELL, J.B.; WARD, G., Volume 1, pp. 1.190-203. Elsevier Applied Science, London/New York, 1992.

[5] VANTORRE, M; ELOOT,K.; HEYLBROECK, B. "Evaluation of mathematical models for propulsion and rudder forces by means of captive model tests with bulkcarriers in shallow water.", International Symposium on Manoeuvrability of Ships at Slow Speed, Itawa, 1995..

[6] CH'NG, P., DOCTORS, L.J. & RENILSON, M.R. A method of calculating the ship-bank interaction forces and moments in restricted waters, *International Shipbuilding Progress*, 1993, **40**, 7-23.

[7] VANTORRE, M. Experimental study of bank effects on full form ship models in: Mini Symposium on Ship Manoeuvrability (Editor: Kijima, K.), pp. 85-101, Fukuoka, 1995, The West-Japan Society of Naval Architects, 1995.

[8] NORRBIN,N.H. "Bank Effects on a Ship Moving Through a Short Dredged Channel".10th ONR Symposium on Naval Hydrodynamics 1974

[9] NORRBIN,N.H. "Bank Clearance and Optimal Section Shape for Ship Canals". PIANC Conference Brussel 1985

[10] HENDRICKX, Ph. "Ontwikkeling van een stuurautomaat voor navigatie op het kanaal Gent-Terneuzen

[11] LAFORCE, E., "Simulator-assisted-design of Harbour renovation: a case study", 10th International Harbour Congress, Antwerp, 1992.

[12] LAFORCE, E.,; VANTORRE,M. "Scheepsmodellen voor scheepsmaneuvreersimulatie". Tijdschrift Openbare werken, nr 6, Brussel 1989.

[13] LAFORCE, E ; CLAEYSSENS P. "Model 515/2 Kanaal Gent-Terneuzen. Risico-analyse schepen 265 m." Min. Flemish Community. Dept. of the Environment & Infrastructure. Waterways Administration. Flanders' Hydraulics. Internal report (in Dutch).Antwerp, 1995.